Dynamic cross-flow electro-Fenton process coupled to anodic oxidation for wastewater treatment: application to the degradation of acetaminophen

Hugo Olvera-Vargas, Jean-Christophe Rouch, Clémence Coetsier, Marc Cretin, Christel Causserand

Dynamic cross-flow electro-Fenton process coupled to anodic oxidation for wastewater treatment: Application to the degradation of acetaminophen

Hugo Olvera-Vargas[a], Jean-Christophe Rouch[a], Clémence Coetsier[a,*], Marc Cretin[b], Christel Causserand[a]

[a] Laboratoire de Génie Chimique, CNRS, INPT, UPS, Université de Toulouse, 118 route de Narbonne, F-31062 Toulouse, France
[b] IEM, Univ Montpellier, CNRS, ENSCM, Montpellier, France

Keywords:
Electro-Fenton
Electrocatalytic membranes
Sub-stoichiometric Ti_4O_7 anode
Membrane technology
Acetaminophen

A B S T R A C T

In this work, we present an integrated dynamic cross-flow electro-Fenton (DCF-EF) system for the treatment of the pharmaceutical, acetaminophen (paracetamol), in aqueous medium. A carbonaceous electrocatalytic membrane was used as cathode, allowing the continuous production of H_2O_2 during EF in dynamic filtration mode. The transmembrane pressure (TMP) and current were the two driving forces of the system, whose influence strongly affected the global efficiency. It was found that H_2O_2 production from the electrochemical reduction of dissolved O_2 was favoured at higher TMP values as a consequence of an increase of the O_2 partial pressure, and higher H_2O_2 amounts entailed an increase in the efficiency of the process. Current also had a positive effect on H_2O_2 production and acetaminophen degradation and mineralization efficiencies up to an optimal value. Complete degradation of the drug and 44% mineralization were achieved under optimal conditions (2.0 bar and 100 mA). On the other hand, the results pointed out that the use of a Ti_4O_7 rod as counter electrode (anode) had an important contribution to the mineralization of the acetaminophen's solutions owing to the formation of hydroxyl radicals (˙OH) on its surface, which highlighted the oxidative power of this anode material. The oxidation mechanisms involved during the process were assessed by electrochemical measurements with both electrodes (carbon membrane and Ti_4O_7 rod), and a degradation pathway for paracetamol oxidation was proposed based on the identification of the main aromatic and aliphatic degradation by-products. This DCF-EF process is presented as a potential alternative for water treatment and reuse in which the integration of membrane and electrochemical technologies brings together separation science and advanced oxidation.

1. Introduction

The critical worldwide water situation demands the development of more efficient and sustainable technologies for wastewater treatment [1]. In this scenario, the unambiguous presence of a variety of persis tent organic pollutants (POPs) in the aquatic environment has boosted research in the field of wastewater treatment during the last decades [2,3]. POPs are substances refractory to conventional physicochemical and biological degradative treatment methods, and physical processes such as membrane filtration, adsorption and coagulation/flocculation are separation technologies that do not involve structural changes. POPs include pharmaceuticals, personal care products, industrial che micals, pesticides and so on. Some organic pollutants of this kind are categorized as contaminants of "emerging concern" because they have only been recently detected in the environment.

Advanced oxidation processes (AOPs) are powerful technologies that were developed for the degradation of refractory contaminants. They are based on the production of highly reactive species, mainly hydroxyl radicals (˙OH), which are capable of mineralizing the organic matter present in the wastewater [4,5]. When AOPs are performed by means of electrochemistry (EAOPs), numerous advantages arise, such as high efficiency, operability at mild conditions, economic feasibility, ease of automation and environmental compatibility. These character istics have positioned them as potential alternatives for large scale applications [6,7]. However, some EAOPs intrinsic limitations still re strain further industrial implementation; mainly the stability and ele vated costs of the electrode materials, mass transport restrictions, re actor design and other engineering issues [6 10].

EAOPs include direct electrochemical oxidation methods, com monly referred as anodic oxidation (AO), and indirect electro oxidation (IEO). AO is based on the electrochemical oxidation of organics at the anode surface through two different mechanisms: (i) direct electron

* Corresponding author.
E-mail address: coetsier@chimie.ups-tlse.fr (C. Coetsier).

https://doi.org/10.1016/j.seppur.2018.03.063

transfer and (ii) indirect oxidation via the "chemisorbed oxygen" (M(˙OH)) formed from water discharge (Eq. (1)). The oxidative mechanism depends on the characteristics of the anode material [6,7,11] and boron doped diamond (BDD) electrodes are the most efficient and preferred materials for AO [11–13]. On the other hand, in recent years Ti_nO_{n-1} (n ≥ 3) sub stoichiometric ceramic anodes, specially Ti_4O_7, have emerged for water remediation applications due to their ability to generate "quasi free" M(˙OH) via Eq. (1) in a similar way to BDD [14–16]. In recent publications, Ti_4O_7 anodes have even been reported to show similar or better performances than BDD [17,18,19]. However, little research on these ceramic materials has been conducted so far. TiO_2 based materials are another type of electrodes commonly used in photoelectrocatalytic EAOPs, in which the photocatalytic oxidative properties of TiO_2 are enhanced by the application of an external bias potential [20].

Because of its numerous advantages, electro Fenton (EF) has received especial attention among the IEO techniques and several studies have evidenced its potentiality [21–25]. The EF process is characterized by the *in situ* cathodic production of the Fenton's reagent: H_2O_2 is formed through the 2 e^- reduction reaction of soluble O_2 at a suitable electrode material (Eq. (2)), while Fe^{2+} is constantly regenerated via Eq. (4). In this way, ˙OH are continuously formed in the bulk solution via the Fenton's reaction (Eq. (3)). The efficiency of the process is highly dependent on the properties of the cathode material [6,21] and generally, carbonaceous electrodes have been used in EF, including gas diffusion electrodes (GDE), carbon felt (CF), graphite, carbon nanotubes (CNT), reticulated carbon vitreous (RCV), carbon fibers, graphene, etc. [6,9,21,26–28]. Additionally, the performance of EF can be enhanced when powerful anodes promoting the generation of M(˙OH) (Eq. (1)) like the BDD are utilized in the same system [29,30].

$$M + H_2O \rightarrow M(^{\bullet}OH) + H^+ + e \quad (1)$$

$$O_2 + 2H^+ + 2e \rightarrow H_2O_2 \quad (2)$$

$$H_2O_2 + Fe^{2+} \rightarrow Fe^{3+} + OH + {}^{\bullet}OH \quad (3)$$

$$Fe^{3+} + e \rightarrow Fe^{2+} \quad (4)$$

On the other hand, single water treatment methods encounter several difficulties, mostly related to technical unavailability and incomplete removal of target pollutants. Therefore, combined or integrated technologies have been increasingly applied over the last years, in which the main advantages of individual processes are enhanced by the beneficial effects of their counterpart, while their downsides are overcome [4,7,31]. In this way, a great variety of coupled systems have been proposed, in which AOPs (including electrochemical methods) have been privileged for the partial or total destruction of organic pollutants during pre or post treatment stages [4,32,33].

In this scenario, Membrane technology (MT) AOPs systems have been applied for the treatment of different organic pollutants with satisfactory results, as recently reviewed by Ganiyu et al. [33]. AOPs as pre treatment have been usually applied with the goal of removing fouling agents, while highly charged concentrates can be efficiently post treated by AOPs/EAOPs [34]. The utilization of anti fouling photocatalytic membranes (TiO_2 based) has become an attractive alternative since physical separation and chemical oxidation can occur in a single unit during "one step" treatments [33,35]. The use of electrocatalytic membranes in integrated MT EAOPs systems has been proposed in more recent works, where the membrane acts as both, separation barrier for filtration and electrode material for the oxidation of organics [36]. Different materials have been used as reactive electrochemical membranes: Ti/BDD [37,38], carbon based membranes [39–42] and sub stoichiometric Ti_4O_7 [43,44]. Nonetheless, the reports available are still scarce and great efforts are needed for improvement.

In precedent investigations, graphite based tubular membranes have been utilized as electrodes for the electrochemical generation of H_2O_2 during EF in dynamic filtration mode, demonstrating the potentiality of this innovative hybrid technique [39]. In fact, carbon based membranes have found a wide range of applications (mainly the separation of gasses and pesticides) because of their high chemical stability and thermal resistance, as well as their good permeability and selectivity [45]. Furthermore, various studies have demonstrated the great potential of carbon membranes as electrodes due to their anti fouling capacity [46]. A recent work reported the use of a membrane with a polymer coating film which promoted the electrochemical formation of ˙OH via the EF process. However, the polymer layer was supported on a steel mesh with poor filtration capacity, which was subjected to corrosion issues [47].

In the present study, we thoroughly investigated the application of an electrocatalytic graphite membrane as cathode for the electro production of the Fenton's reagent during a combined dynamic cross flow EF process (DCF EF) at pre pilot scale. Paracetamol (PCTM), a widely prescribed analgesic and antipyretic drug, whose unequivocal presence in surface, drinking and wastewater has been stated worldwide, was used as model compound. The main parameters affecting the efficiency of the process, named applied current and transmembrane pressure (TMP), were systematically assessed. Furthermore, a "non active" Ti_4O_7 anode was used as the counter electrode during EF in filtration mode for the very first time, which resulted in a significant rise of efficiency. The mechanisms involved in the oxidation of the drug were deeply investigated and a plausible degradation pathway was proposed based on the identification of degradation by products.

2. Materials and methods

2.1. Membrane characterization

The conductive membrane used as cathode was a graphite based ultrafiltration membrane from Carbone Lorraine, France, with dimensions: 15 cm long, 1 cm outer diameter and 0.8 cm inner diameter. Before utilization, it was washed in deionized water, sonicated, washed with acetone for removal of any organic remnant, overnight in 0.05 M H_2SO_4 and finally immersed in deionized water for hydration (24 h). The extremes were covered with epoxy resin for sealing inside the cell/filtration module (2 and 4 cm each extreme) and the effective inner membrane area was 22.62 cm^2. Membrane porosity was found to be 14.4% according to Hg measurements, while it has a pore diameter of 2.8 and 0.16 μm, according to previous study [39].

2.2. EF Membrane cross flow electrolyses

The electrochemical filtration pre pilot scale reactor used in this study is depicted in Fig. SM 1. Experiments were conducted in cross flow filtration mode under galvanostatic conditions using a DC 30 V/10 A power supply. The reservoir consisted in a 5 L capacity stainless steel tank, in which aqueous solutions of PCTM (0.1 mM) were introduced and circulated by a centrifugal pump at a flow rate of 3 L min^{-1}. The tank was equipped with a cooling system for temperature control and a temperature sensor for monitoring. The electrolytic cell/filtration module was a tubular Teflon® container, which held the graphite membrane (cathode). It had an outlet for the permeate, which was not recirculated. The external wall of the membrane was connected to the power supply by a metallic contact. The counter electrode (anode) consisted of a 1 mm diameter, 30 cm long Ti/Ti_4O_7 rod. It was placed in the axis of the carbon membrane and connected to the supply power by the extremity. Transmembrane pressure (TMP), the driving force of MT, was adjusted using compressed air, which also ensured continuous supply of O_2 for saturation of the solution. For all experiments, the electrolysis started after the system had reached a permanent regime and the concentration of PCTM in the permeate was constant (adsorption was negligible). The solution was saturated with O_2 during the stabilization time. All experiments were replicated and the average

values are reported.

2.3. Ti_4O_7 anode preparation

The preparation of the Ti_4O_7 anode (rod) was made by the method described in a precedent work, where the deposition of TiO_x particles was effectuated by plasma coating on titanium plates as support [18]. In this case, the plasma coating was made by Saint Gobain Coating Solutions on a 30 cm titanium rod (1 mm diameter) using their Pro Plasma STD plasma torch. X ray Diffraction (XRD) analyses revealed that Ti_4O_7 was the main phase of the plasma coating. Saint Gobain CREE synthesized the TiO_x particles by electrofusion using a Heroult furnace in which a mixture of TiO_2 and coke (Coke de Brai AO151203 ALTICHEM 98% C) was melt by the electric arc created between gra phite electrodes. XRD of the obtained powder revealed a mixture of Ti_4O_7, Ti_5O_9, Ti_6O_{11} and Ti_3O_5 phases.

2.4. Analytic techniques and instrumentation

HPLC analysis for PCTM quantification were performed in a HPLC UV Agilent 1200 series chromatograph couple to a UV detector set at 240 nm. An Agilent reversed phase C18 column (3.5 µm × 100 mm × 3 mm) was used. The mobile phase consisted of A (0.1% formic acid aqueous solution) and B (0.1% formic acid in acet onitrile). The gradient program used for elution at a flow rate of 1.2 mL min^{-1} was as follows: 0 3.5 min (isocratic 97.5/2.5), 3.5 6.5 min (gradient up to 20/80), 6.5 7.5 (gradient up to 97.5/2.5) and 7.5 10.5 (isocratic 97.5/2.5). Quantitation of short chain car boxylic acids was made using an HPLC Jasco BS 2000 04 equipped with a UV 2077 detector. An Agilent Hi Plex H column was used (7.7 × 300 mm, 8 µm) and elution was performed with 0.01 M H_2SO_4 at a flow rate of 0.4 mL min^{-1} and 50 °C. Detection was made at 210 nm. The mineralization rate was assessed in terms of the TOC decay in the treated solutions. TOC analyses were carried out using a Shimadzu V_{CSH} TOC analyser.

HPLC HRMS analyses were performed in a Thermo Fisher instru ment (U3000). HPLC separations were carried out at 40 °C using a Luna PFP 2 (150 × 2 mm, 3 µm) column. The mobile phase was an A (0.1% v/v formic acid)/B (acetonitrile) mixture, while the gradient program at 200 µL min^{-1} was: 0 5 min (100/0), 5 20 min (gradient up to 20/ 80), 20 25 min (20/80), 25 25.2 min (gradient up to 100/0), 25.2 30 min (100/0). In parallel, analyses were performed using UV detection (UV Vis RSLC VWD 3400 RS detector) at 250 nm. The MS spectrometer is combined with an Orbitrap mass analyser. It is equipped with an HCD collision cell, using electrospray ionization (ESI), which was operated in positive and negative mode. Mass detec tion was made between 50 and 600 *m/z*. Biological oxygen demand at 5 days (BOD_5) was determined using an OxiTop® system. The samples, in which pH was adjusted to a value between 6.5 and 7.5, were in cubated at 20 °C in dark conditions during 5 days. KOH pellets were used to trap CO_2. BOD seed inoculum (PolySeed®, Interlab® Supply) was used as source of microorganisms, while D(+) Glucose H_2O was the standard control and N allylthiourea was utilized as nitrification in hibitor. H_2O_2 was quantified by spectrophotometry with $TiCl_4$ at 410 nm using a UV vis Libra S12 Biochrom spectrophotometer [48].

The voltametric studies were performed on an Autolab PGSTAT204 potentiostat/galvanostat at a scan rate of 50 mV s^{-1} using a Ag/AgCl reference electrode. The electrolytic cell for the batch experiments re ported in Section 3.4, was a 200 mL glass tall container equipped with either a Ti_4O_7 rod or a fstainless steel rod (316 L stainless steel with excellent corrosion resistance) as anode, while the cathode was a Pt mesh; 21 cm of both electrodes were immersed in the solution (200 mL). The cell for the electrochemical characterization of the gra phite membrane, reported in Section 3.1, consisted in a 200 mL capa city reactor, containing a 7 cm long carbon tubular membrane as cathode and a Pt mesh anode (5 cm immersed in the solution, 150 mL).

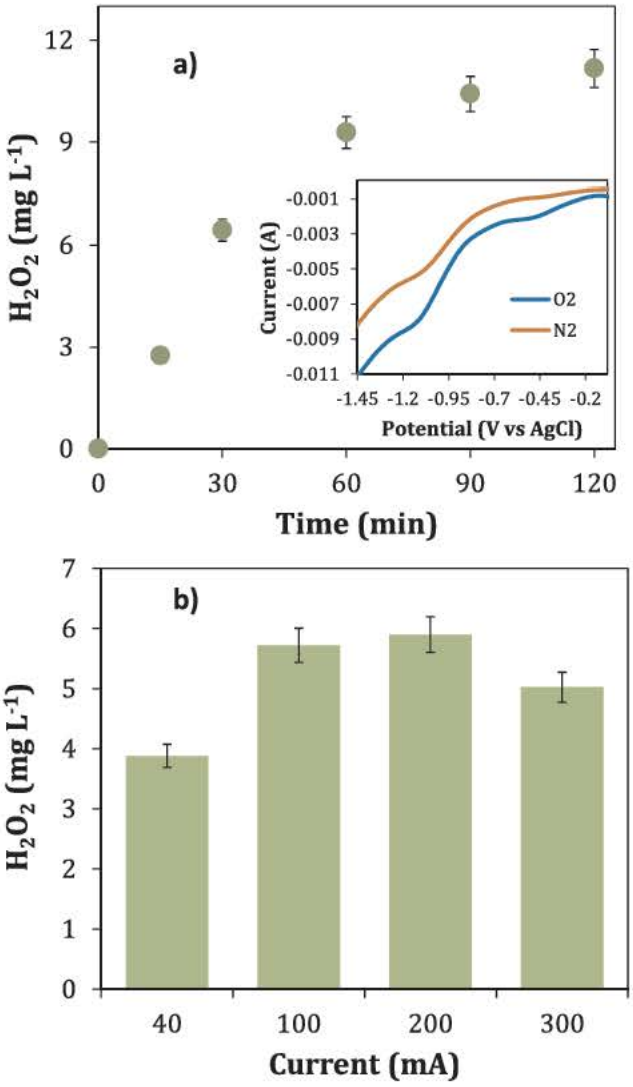

Fig. 1. Effect of applied current on the electrochemical production of H_2O_2. (a) evolution of H_2O_2 with electrolysis time (at 100 mA). (b) Concentration of H_2O_2 at 30 min-electrolysis under different current values. V = 1.5 L of 0.05 M Na_2SO_4 at pH 3 ,18 °C and 0.25 bar. Flow = 3.0 L min^{-1}. The inset panel de- picts the linear voltammogramm of the electrolyte solution (0.05 M Na_2SO_4 at pH 3) in the presence (O_2) and absence of O_2 (N_2).

Before experiments, the solution was saturated with O_2 for 15 min using compressed air. For both cells, the anode and the cathode were installed in parallel in the center of the cell, separated by 1 cm. Na_2SO_4 50 mM at pH 3 was used as a supporting electrolyte.

3. Results and discussion

3.1. H_2O_2 electro generation: effect of TMP and current

TMP and current are the driving forces of this coupled DCF EF process. Accordingly, the effect of both parameters was assessed: first, on the generation of H_2O_2 and second, on PCTM degradation and mi neralization efficiencies.

The use of a graphite based membrane ensured the electrochemical production of H_2O_2 from the 2 e^- reduction reaction of dissolved O_2 in the solution. The formation rate of H_2O_2 depends on the structure and properties of the cathode material since O_2 reduction can occur through either the 2 e^- or the 4 e^- reaction pathway (Eqs. (2) and (5), re spectively), the latter leading to H_2O generation [21]. Linear Sweep Voltammetry (LSV) was used to assess the electrochemical reduction

reaction of O_2 in the tubular membrane. The inset panel of Fig. 1 depicts the linear voltammogram of the supporting electrolyte (Na_2SO_4) saturated with O_2 at pH 3. Two reduction waves before the evolution of H_2 can be observed at −0.47 V and −1.1 V *vs* Ag/AgCl, which correspond to the 2 e^- O_2 reduction reaction (ORR) (Eq. (2)) and the consecutive 2 e^- reduction of H_2O_2 (Eq. (6)), respectively. These results confirmed the formation of H_2O_2.

$$O_2 + 4H^+ + 4e \rightarrow 2H_2O \quad (5)$$

$$H_2O_2 + 2H^+ + 2e \rightarrow 2H_2O \quad (6)$$

Since current is a crucial parameter for the electro production of H_2O_2 and the generation of $^{\cdot}OH$ in the presence of Fe^{2+} ions (Fenton's reaction), its effect on H_2O_2 production was assessed by a series of experiments at different current values, ranging from 40 to 300 mA (1.77 mA cm^{-2} to 13.26 mA cm^{-2}). It was found that the concentration of H_2O_2 in the feed increased with time until a plateau was reached, which is illustrated in Fig. 1a. It can be seen that a maximum of 11 mg L^{-1} was obtained after 90 min electrolysis (at 100 mA). Fig. 1b depicts the generation of H_2O_2 as a function of current at 30 min electrolysis. The rate of H_2O_2 production rose with increasing current from 40 to 200 mA, but decreased at higher current values (300 mA). This trend was in agreement with the electrochemical behaviour of the ORR at the cathode membrane (inlet Fig. 1), according to which higher current values (requiring higher potentials) contribute to the progressive decomposition of H_2O_2 into H_2O (Eq. (5)). The experiments were conducted under constant current since it is known that galvanostatic mode is preferred for large scale applications due to the slow kinetics obtained under potentiostatic conditions [7].

TMP is the other driving force of this coupled process. Accordingly, its effect on the generation of H_2O_2 was also investigated. For this purpose, a series of electrolyses were performed at pressures ranging from 0.5 to 2.0 bars (Fig. 2). It can be seen that TMP has a positive effect on the generation of H_2O_2. This phenomenon can be explained in terms of the increase in O_2 solubility in water as a function of its partial pressure according to Henry's law. Thereby, a greater amount of O_2 dissolved in the solution increases the mass transport of the gas to the electrode, favouring the generation rate of H_2O_2. In Fig. 2, the amount of H_2O_2 is presented as a function of TMP and the equivalent amount of dissolved O_2 calculated from Henry's law according to the corresponding O_2 partial pressure. Similarly, in a recent study the electrochemical production of H_2O_2, as well as the performance of the EF

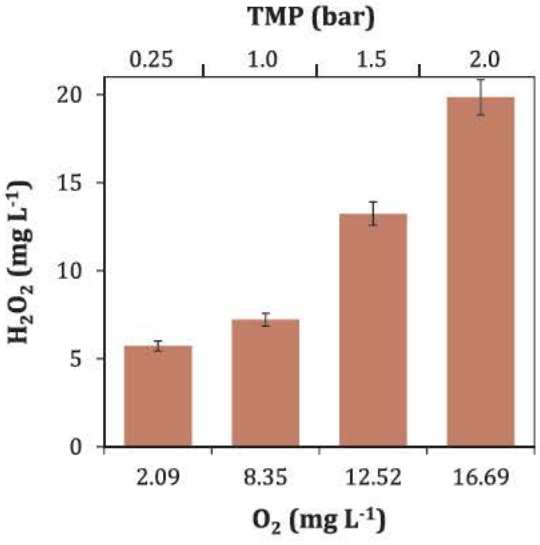

Fig. 2. Effect of TMP (and the corresponding O_2 concentration as a function of its partial pressure) on the electrochemical production of H_2O_2 at 30 min of electrolysis of 1.5 L of 0.05 M Na_2SO_4 at pH 3 and 18 °C. Flow = 3.0 L min^{-1}.

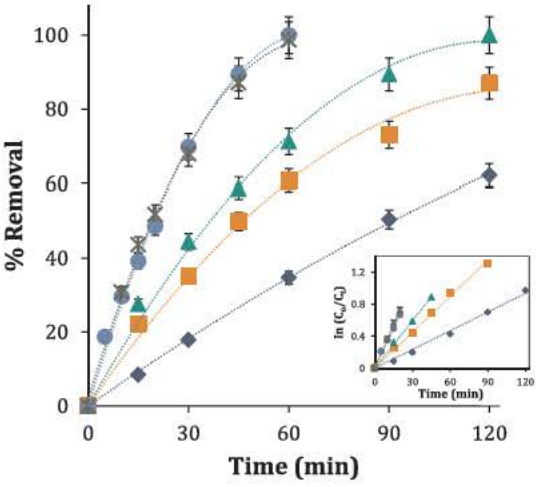

Fig. 3. Effect of TMP on the degradation of PCTM during DCF-EF. V = 1.5 L, [PCTM] = 0.1 mM, [Fe^{2+}] = 0.2 mM, I = 100 mA, with 0.05 M Na_2SO_4 at pH 3 and 18 °C. Flow = 3.0 L min^{-1}. (■) 0.25 bar, (▲) 1.0 bar, (●) 2.0 bar, (*) 3.0 bar, (♦) 0.25 bar in the absence of Fe^{2+} (AO). The inset panel shows the kinetic analysis assuming a pseudo-first order model.

process, were enhanced by increasing the air pressure in a pressurize electrolytic cell operating in batch mode [49]. This phenomenon is of noticeable importance since it highlights the synergistic effects of EF under pressure driven filtration mode. Therefore, further deposition of ultra or nanofiltration layers on the carbon membrane support, associated with greater TMP values, will be compatible with EF oxidation.

3.2. Degradation and mineralization kinetics

3.2.1. Effect of TMP

The effect of TMP and current on the degradation and mineralization of PCTM aqueous solutions under DCF EF conditions was also assessed. Fig. 3 depicts the drug's removal percentage with time at different TMP values. As expected, an increment in TMP resulted in a rise in the degradation kinetics, which is consistent with the greater production of H_2O_2 from the increase of O_2 solubility in solution. Accordingly, larger amounts of H_2O_2 promoted an extensive generation of $^{\cdot}OH$ from Fenton's reaction (Eq. (3)), which accelerated the oxidation rate of the drug. The removal rate increased with TMP from 0.25 to 2.0 bars, while it did not show any further increase when 3.0 bar were applied. This behaviour can be accounted for by the catalytic capacity of the membrane with regard to the 2 e^- ORR, which limited the formation of H_2O_2 even at higher levels of pressure. A total degradation of the drug was achieved in 60 min for a TMP of 2.0 and 3.0 bar, while PCTM was totally degraded in 90 and 120 min when using 1.0 and 0.25 bar, respectively. In addition, we hypothesize that adsorption of organics on the membrane played an important role on the electrocatalytic activity for H_2O_2 production. In this way, saturation of the membrane conducted to electrode passivation, which accounted for the decrease in the oxidation rates with time.

On the other hand, the degradation kinetic of the drug was found to follow a pseudo first order kinetic model with very good correlation coefficients, as shown in the inset panel of Fig. 3. This behaviour was in agreement with reported kinetic rates of organics with $^{\cdot}OH$, in which a quasi stationary state in the concentration of this species has been considered. Table 1 summarizes the calculated pseudo first order rate constants ($k_{app,PCTM}$).

Concerning the mineralization of the drug, it can be seen from Fig. 4 that TMP also had a positive effect on the TOC decay of PCTM solutions. The application of 2.0 and 3.0 bar resulted in up to 44% of mineralization. On the other hand, the contribution of AO on the total mineralization yield is noteworthy. Fig. 4 shows that 19% of TOC decay was achieved in the

Table 1
Apparent rate constants for the complete disappearance of 0.1 mM PCTM by means of the DCF-EF process: effect of TMP and current. A pseudo-first order kinetic model was assumed.

Experimental parameters	Values	$k_{app,PCTM}$ (min ^{1})
TMP (bar)	0.25	0.015
(I = 100 mA)	1.0	0.020
	2.0	0.034
	3.0	0.037
	0.25 (AO)[a]	0.008
Current (mA)	40	0.005
(TMP = 0.25 bar)	100	0.011
	200	0.016
	300	0.019

[a] For AO the experiment was conducted in the absence of Fe^{2+} ions.

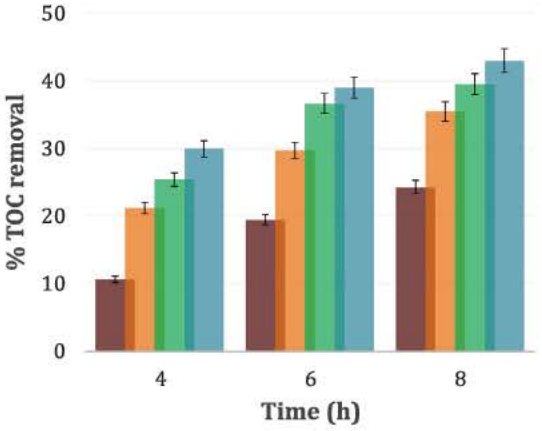

Fig. 4. Effect of TMP on the TOC decay of PCTM solutions during DCF-EF. V = 1.5 L, [PCTM] = 0.1 mM, [Fe^{2+}] = 0.2 mM, I = 100 mA, with 0.05 M Na_2SO_4 at pH 3 and 18 °C. Flow = 3.0 L min^{-1}. (■) 0.25 bar in the absence of Fe^{2+} (AO), (■) 0.25 bar, (■) 1.0 bar, (■) 2.0 bar.

absence of Fe^{2+} ions, which evidenced that an important part of PCTM and its degradation by products were mineralized on the anode's surface by means of the M(˙OH) formed according to Eq. (1). These results highlighted the potential of Ti_4O_7 anode materials for water remediation. Further discussion is presented in Section 3.4.

3.2.2. *The effect of current*

The effect of current on the performance of DCF EF is depicted in Fig. 5. It can be observed that the concentration decay rose with current from 40 to 200 mA, with a small difference between 100 and 200 mA. Nevertheless, it decreased when 300 mA were applied. The increase in the kinetic rate with current was due to the greater amount of ˙OH produced from both the Fenton's reaction (Eq. (3)) and water oxidation (Eq. (1)) as a consequence of a higher energy input. On the contrary, further increment of current entailed progressive acceleration of non oxidizing waste reactions: the heterogeneous electrochemical evolution of O_2 at the anode (Eq. (7)), the reduction of H_2O_2 at the cathode (Eq. (6)), the homogeneous dimerization of ˙OH (Eq. (8)), and ˙OH reaction with Fe^{2+} and H_2O_2 according to Eqs. (9) and (10), respectively [8,21].

$$M(^{\bullet}OH) \rightarrow 2\ M + O_2 + 2H^+ + 2e \quad (7)$$

$$2^{\bullet}OH \rightarrow H_2O_2 \quad (8)$$

$$Fe^{2+} + {}^{\bullet}OH \rightarrow Fe^{3+} + OH \quad (9)$$

$$H_2O_2 + {}^{\bullet}OH \rightarrow HO_2^{\bullet} + H_2O \quad (10)$$

As shown in Fig. 6, TOC decay behaves in a similar way. The mineralization rate increased when rising current from 40 mA to 100 mA, whereas the difference between 100 and 200 mA was not significant

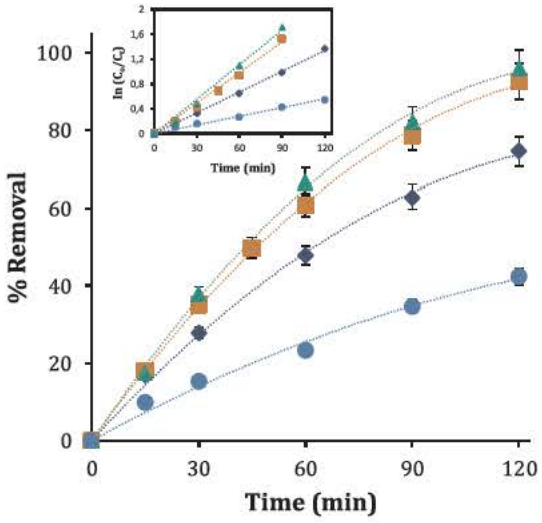

Fig. 5. Effect of current on the degradation of PCTM during DCF-EF. V = 1.5 L, [PCTM] = 0.1 mM, [Fe^{2+}] = 0.2 mM, TMP = 0.25 bar, with 0.05 M Na_2SO_4 at pH 3 and 18 °C. Flow = 3.0 L min^{-1}. (♦) 40 mA, (■) 100 mA, (▲) 200 mA, (●) 300 mA. The inset panel shows the kinetic analysis assuming a pseudo-first order model.

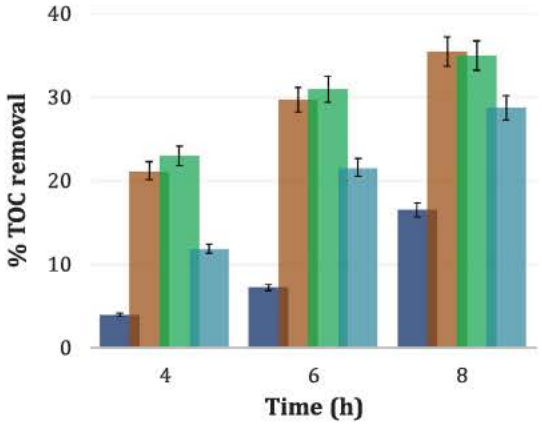

Fig. 6. Effect of current on the TOC decay of PCTM solutions during DCF-EF. V = 1.5 L, [PCTM] = 0.1 mM, [Fe^{2+}] = 0.2 mM, TMP = 0.25 bar, with 0.05 M Na_2SO_4 at pH 3 and 18 °C. Flow = 3.0 L min^{-1}. (■) 40 mA, (■) 100 mA, (■) 200 mA, (■) 300 mA.

(35% of TOC decay was reached after 8 h of treatment for both, 100 and 200 mA). The application of 300 mA resulted in a significant drop of mineralization efficiency, which can be accounted for by the series of waste reactions depicted in Eqs. (6) (10), as discussed above.

It can be noted that TOC decay rates decrease with treatment time. For example, for 100 and 200 mA, more than 20% of TOC abatement was reached in 4 h electrolysis, whereas, only around 12% more was achieved during the next 4 h. This trend can be ascribed to the gen eration of more recalcitrant degradation by products to ˙OH, whose reaction rates are significantly slower. These compounds include mostly short chain organic acids. Further discussion is proposed in Section 3.5.

Finally, even though retention was not involved during CF EF, the re levance of these carbonaceous electrocatalytic membranes in EF is to be underlined as the filtration properties can be improved by deposition of ultra and nano filtration layers. Additionally, the efficiency of the mem branes towards the 2 e$^-$ O_2 reduction reaction could also be improved by structural modifications with graphene [26,50] or nitrogen based com pounds [51] to increase the H_2O_2 production. For these purposes further research needs to be conducted, which was not the scope of the present investigation.

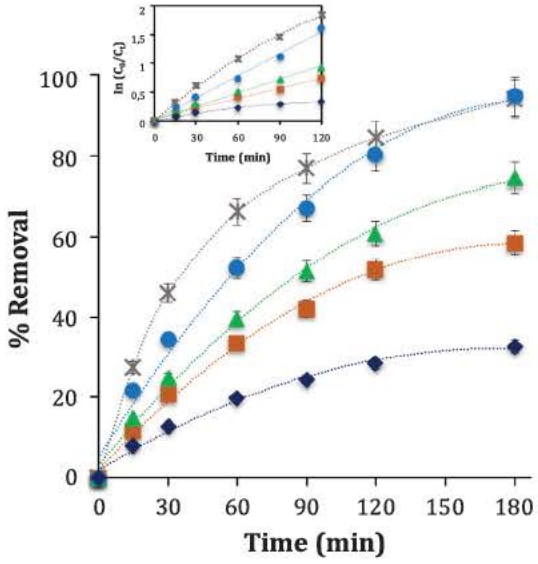

Fig. 7. Effect of current on the degradation of PCTM during AO in batch mode using a Ti_4O_7 anode and a Pt cathode. V = 0.2 L, [PCTM] = 0.1 mM, with 0.05 M Na_2SO_4 at pH 3 and room temperature. (♦) 40 mA, (■) 100 mA, (▲) 200 mA, (●) 300 mA, (*) 100 mA using a stainless-steel anode. The inset panel shows the kinetic analysis assuming a pseudo-first order model.

3.3. The oxidation power of TiOx

In order to assess the mineralization power of the Ti_4O_7 electrode, a series of experiments were conducted in an electrolysis cell operating in batch mode. The cell was equipped with a Ti_4O_7 anode and a Pt cathode in either a three or two electrodes configuration. The use of Pt allowed avoiding the cathodic production of H_2O_2. It was found that the con centration decay of the drug followed a pseudo first order kinetic re action and the degradation rate increased with rising current (Fig. 7), which was consistent with findings obtained in the DCF EF reactor.

When using a stainless steel anode instead of the Ti_4O_7 in the same batch cell, the concentration of the drug decreased with time also fol lowing a pseudo first order kinetic reaction (Fig. 7). In fact, PCTM was oxidized at the surface of the stainless steel anode by direct electron transfer, which, in acidic medium, lead to the formation and accumu lation of p benzoquinone (p BQ), according to Eq. (11) [52]. None theless, according to HPLC analyses (results not presented), p BQ did not suffer further oxidation at prolonged electrolysis time (up to 4 h), which was also reflected in the lack of TOC decrease. In the case of the Ti_4O_7 anode, the concentration of p BQ (determined by HPLC and TOC) decreased with electrolysis time, which confirmed that M(˙OH) medi ated oxidation of PCTM occurred at the Ti_4O_7 electrode's surface. In deed, p BQ is considered as a probe of ˙OH generation since this compound does not undergo direct electrochemical electron transfer reactions [44]. Thus, the use of PCTM in the present study resulted in an *in situ* M(˙OH) probe for the anodic oxidation of organics on Ti_4O_7 electrodes.

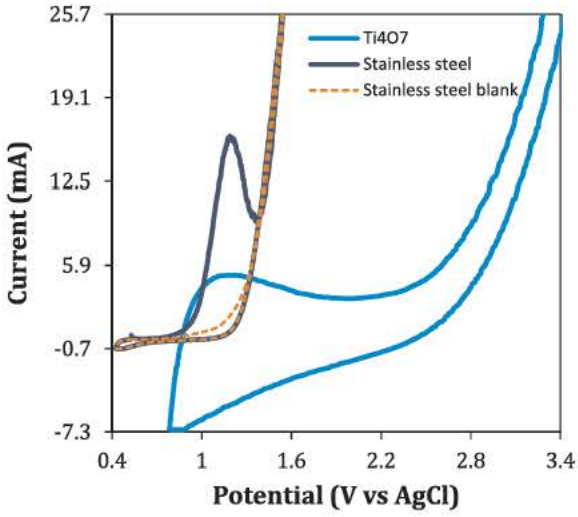

Fig. 8. Cyclic voltammetry of 5 mM PCTM solutions containing 0.05 M Na_2SO_4 at pH 3 as supporting electrolyte. Stainless-steel or Ti_4O_7 were used as anodes with a Pt cathode using a Ag/AgCl reference electrode. The scan rate was 50 mV s^{-1}.

Fig. 8 depicts the cyclic voltammograms of PCTM solutions in 50 mM Na_2SO_4 at pH 3 using Ti_4O_7 and stainless steel anodes. On stainless steel anode, an oxidation wave can be seen at +1.18 V *vs* Ag/AgCl, which corresponds to the irreversible oxidation of PCTM to p BQ (Eq. (11)). On the contrary, any oxidation wave was observed when utilizing Ti_4O_7, which was in agreement with the slow kinetics of electron transfer reactions reported for this kind of material [14,17]. PCTM was thus oxidized by ˙OH formed in the region of O_2 evolution (+2.7 V *vs* Ag/AgCl). The generation of ˙OH in sub stoichiometric Ti_4O_7 electrodes (Ebonex@) was previously verified by Bejan et al. [17]. Moreover, it is known that Ebonex@ anodes have a very high O_2 evolution overpotential [14]. Additionally, the electrolysis of a 0.1 mM solution of p BQ was performed utilizing a divided cell with a Ti_4O_7 anode. Results showed that p BQ was totally degraded in the anodic compartment and up to 20% of mineralization was achieved after 8 h electrolysis at 100 mA, hence confirming the oxidation of p BQ by mediation of heterogeneous Ti_4O_7(˙OH). The slow kinetics for p BQ degradation and mineralization can be explained by: (1) the small surface area of the electrode (5.35 cm^2 for 200 mL of p BQ solution), and (2) the relative less abundance of ˙OH at the Ti_4O_7 anode in comparison to those formed at BDD, as suggested in earlier investiga tions [17].

3.4. PCTM oxidation pathway

Aiming at establishing the mechanism reaction through which PCTM is oxidized during DCF EF, the degradation intermediates were identified by means of HPLC and HPLC MS analysis (Table SM 1). Fig. 9 depicts the proposed mechanism pathway. As mention in the previous section, PCTM is oxidized both in the bulk solution with ˙OH formed by

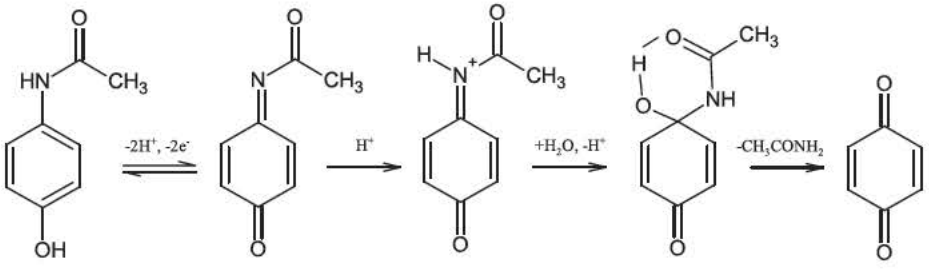

(11)

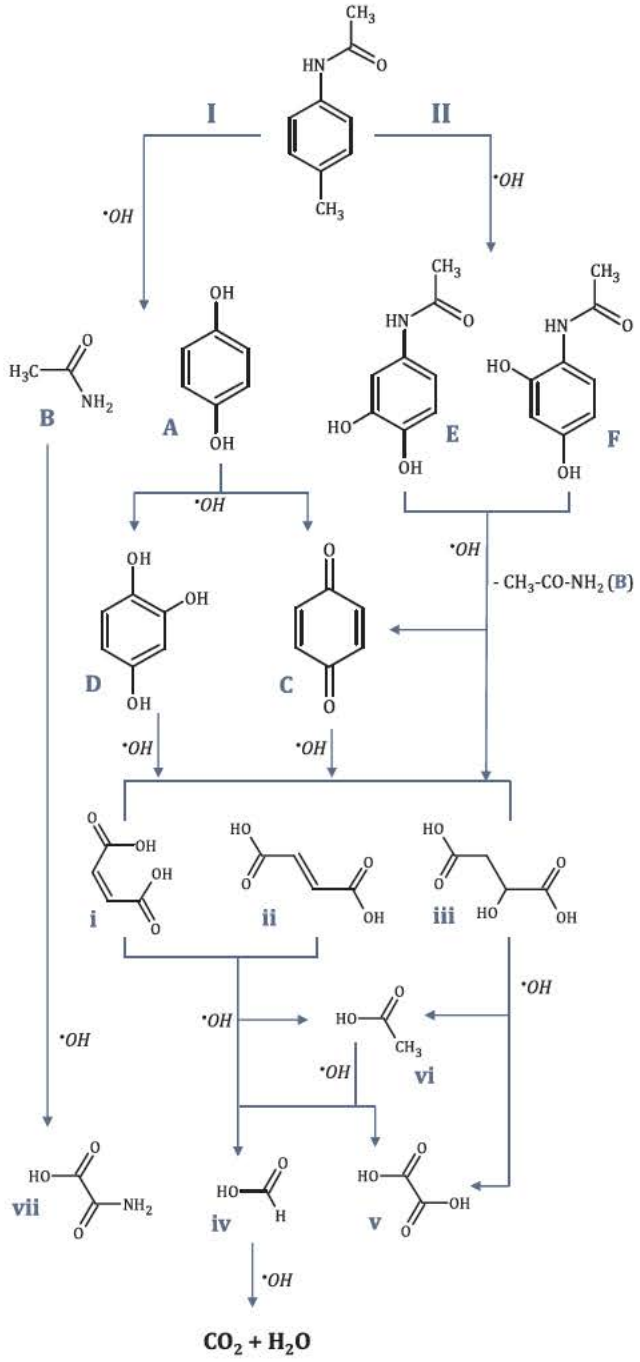

Fig. 9. Proposed mechanisms pathway for the oxidation of PCTM with ˙OH during the DCF-EF process.

Fenton's reaction (Eq. (3)) and at the surface of the anode with Ti_4O_7(˙OH) (Eq. (1)). The HPLC chromatograms showed that p BQ was the degradation by product produced in greatest amount, but it was also degraded as the treatment progressed. As depicted in Fig. 9, PCTM oxidation began with hydroxylation at the *p* position with respect to the OH group, which gave first hydroquinone (HQ) (A) and acetamide (B) (route I). Quick subsequent oxidation of HQ generated p BQ (C) as the principal product. However, HQ also underwent further hydroxylation reactions, which was verified by the detection of 1,2,4 trihydroxybenzene (D). On the other hand, formation of 4 acetyl aminocatechol (E) and 4 acetyl aminoresorcinol (F) revealed that hydroxylation reactions at the *o* and *m* positions of PCTM (route II) competed with the first hydroxylation path (route I), but at slower kinetic rates. Further

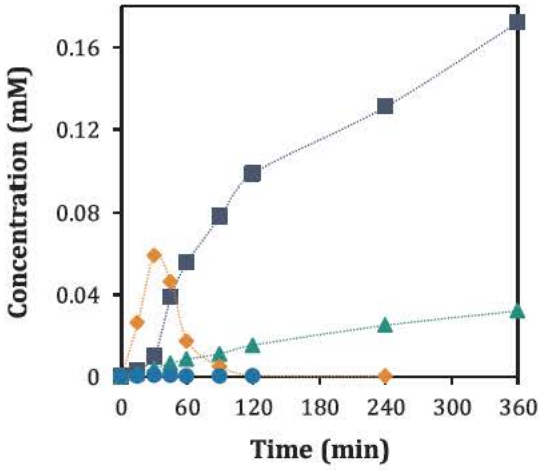

Fig. 10. Evolution of the concentration of the main carboxylic acids formed during the degradation of PCTM by means of DCF-EF. V = 1.5 L, [PCTM] = 0.1 mM, $[Fe^{2+}]$ = 0.2 mM, TMP = 1.0 bar, *I* = 100 mA, with 0.05 M Na_2SO_4 at pH 3 and 18 °C. Flow = 3.0 L min^{-1}. (■) oxalic, (●) malic, (▲) oxamic, (♦) formic.

˙OH attack to the aromatic intermediates C, D, E and F provoked their scission leading to short chain organic acids (i to vii). The cleavage of E and F went through progressive hydroxylation reactions giving quinones (like C) by disproportionation of transient semiquinones. The proposed mechanism is in agreement with previous reports dealing with PCTM degradation by anodic oxidation [53], photo Fenton [54] and photocatalytic oxidation [55]. Moreover, Almeida et al. reported that the photoelectron Fenton oxidation of PCTM in a flow plant also went through formation of HQ and p BQ [56]. However, they did not observe either intermediates (E) and (F) formed through the hydroxylation route II or acetamide (B), which can be ascribed to the fast oxidation kinetics of PCTM and its degradation intermediates. Waterston et al. reported that the electrochemical oxidation of PCTM at Ti/IrO_2 anodes only conducted to partial degradation to p BQ, since this "active" anode does not promote ˙OH generation [57].

It has been well documented that breakage of aromatic/cyclic by products by the attack of ˙OH during EAOPs leads to short chain carboxylic acids [58,59]. The evolution of the identified carboxylic acids during DCF EF is depicted in Fig. 10. Cleavage of intermediates C, D, E and F, led mainly to C 4 maleic (i), fumaric (ii) and malic acids (iii). These compounds were only detected during the first 60 min of treatment and in very low amounts: malic acid reached a maximum peak (7.2×10^{-4} mM) at 30 min. Their further oxidation conducted to lower molecular weight compounds: maleic and fumaric acids are known to produce formic (iv) and oxalic acid (v), while malic acid yielded mainly oxalic acid (v). It has been reported that acetic acid (vi) can be formed from the oxidation of all the above mentioned C 4 acids. However, only a little amount of it was detected during the first 15 min treatment as it was rapidly oxidized into oxalic and formic acids [58]. Oxalic and formic acids were the species formed in greatest amounts. They were rapidly produced and accumulated in the solution as C 4 acids were oxidized. Both species, along with oxamic acid, are known as the ultimate degradation by products before mineralization to CO_2 and inorganic ions [21,58,59]. It can be noted in Fig. 10 that formic acid quickly attained a maximum concentration in 15 min and it was oxidized afterwards until undetectable levels. In the case of oxalic acid, it was progressively formed and accumulated in the solution, remaining even after 8 h treatment. Oxamic acid (vii), which resulted principally from the oxidation of acetamide (B), presented a similar trend. In fact, oxalic and oxamic acids are known to be highly resistant to oxidation with ˙OH, presenting slow reaction kinetic rates [59]. Accordingly, they were the main carbon source responsible for the remaining amount of TOC at the end of treatment, which was verified by a simple TOC mass

balance indicating that 86% of the final TOC content of the treated solution corresponded to oxalic and oxamic acids.

3.5. Final considerations: the positive impact of the degradation by products

It has been stated that the carboxylic acids formed during electrochemical treatment are biodegradable compounds that can be effectively metabolized by different microorganisms [60,61]. Generally, the subsequent oxidation of these species demands longer treatments times owing to their recalcitrant character towards ˙OH. Prolonged electrolyses are typically accompanied by a significant drop in current efficiency and an increment of energy consumption. Nevertheless, the ability of EAOPs to transform recalcitrant compounds into biodegradable products is indeed one of its most significant features since the striking oxidation power of EAOPs can be capitalized by their combination (as pre or post treatment steps) with conventional biological treatment methods. Thus, the short time partial oxidation of refractory effluents achieved during EAOPs can be completed by implementation of a microbial oxidation stage, which represents considerable technical and economic advantages from a practical perspective [32,62]. In this context, the capability of the DCF EF process to transform refractory pollutants into biodegradable compounds is to be underlined.

In addition, the capacity of DCF EF to degrade p BQ is worthy of note since this intermediate is a hazardous compound much more toxic than PCTM. In fact, Le et al. recently reported that p BQ was the main by product responsible for the significant increase of toxicity (according to the Microtox® method) during the EF treatment of PCTM solutions; 100% of bacteria bioluminescence inhibition even at the lowest detected levels of this compound (0.04 mM) was obtained [26]. They reported that the toxicity decreased with the p BQ degradation and the final carboxylic acids did not show significant toxic effects. The elimination of p BQ during DCF EF is in agreement with these results, which highlights the ability of this coupled approach to degrade toxic contaminants.

4. Conclusions

The efficiency and applicability of the one step integrated DCF EF process to the treatment of refractory organic pollutants such as pharmaceuticals has been demonstrated. It was found that the utilization of a graphite based membrane as cathode material was suitable for the electro generation of the Fenton's reagent during electrolysis. TMP and current were the main factors affecting the process efficiency. The results showed that the solubility of O_2 increased as TMP augmented, which promoted greater production of H_2O_2 and a rise of the degradation and mineralization rates. Total degradation of PCTM and up to 44% of mineralization was achieved under optimal conditions (100 mA and 2.0 bar).

The use of a Ti_4O_7 ceramic anode during DCF EF was a highlight of this work. It enhanced the performance of the process due to the M (˙OH) generated on the electrode surface, hence demonstrating the power of Ti_4O_7 for the anodic oxidation of organic contaminants. In addition, PCTM was found to be an *in situ* probe for verification of M (˙OH) formation since its primary oxidation yielded p BQ as the main intermediate, which is known to resist direct electron transfer reactions.

Finally, these findings pointed out the versatility of the EF process, highlighting its capacity to evolve into different directions. Overall, this work opens the door to further investigation for scale up and eventual industrial application of this technology considering the scarce number of reports available to date.

Acknowledgments

This work was supported by The French National Research Agency (ANR) through the grant ANR 13 ECOT 0003 funding, EcoTechnologies et EcoServices (ECO TS) of the CElectrON project: "Electro oxidation and Nanofiltration Coupling for wastewater treatment". The authors acknowledge Dr. David Riboul for the HPLC MS analysis.

Appendix A. Supplementary material

Supplementary data associated with this article can be found, in the online version, at https://doi.org/10.1016/j.seppur.2018.03.063.

References

[1] A.R. Ribeiro, O.C. Nunes, M.F.R. Pereira, A.M.T. Silva, An overview on the advanced oxidation processes applied for the treatment of water pollutants defined in the recently launched Directive 2013/39/EU, Environ. Int. 75 (2015) 33–51, http://dx.doi.org/10.1016/j.envint.2014.10.027.

[2] M.B. Ahmed, J.L. Zhou, H.H. Ngo, W. Guo, N.S. Thomaidis, J. Xu, Progress in the biological and chemical treatment technologies for emerging contaminant removal from wastewater: a critical review, J. Hazard. Mater. 323 (2017) 274–298, http://dx.doi.org/10.1016/J.JHAZMAT.2016.04.045.

[3] M.O. Barbosa, N.F.F. Moreira, A.R. Ribeiro, M.F.R. Pereira, A.M.T. Silva, Occurrence and removal of organic micropollutants: an overview of the watch list of EU Decision 2015/495, Water Res. 94 (2016) 257–279, http://dx.doi.org/10.1016/j.watres.2016.02.047.

[4] I.O. Uribe, A. Mosquera-Corral, J.L. Rodicio, S. Esplugas, Advanced technologies for water treatment and reuse, AIChE J. 61 (2015) 3146–3158, http://dx.doi.org/10.1002/aic.15013.

[5] M.A. Oturan, J.-J. Aaron, Advanced oxidation processes in water/wastewater treatment: principles and applications. A review, Crit. Rev. Environ. Sci. Technol. 44 (2014) 2577–2641, http://dx.doi.org/10.1080/10643389.2013.829765.

[6] F.C. Moreira, R.A.R. Boaventura, E. Brillas, V.J.P. Vilar, Electrochemical advanced oxidation processes: a review on their application to synthetic and real wastewaters, Appl. Catal. B Environ. 202 (2017) 217–261, http://dx.doi.org/10.1016/j.apcatb.2016.08.037.

[7] C.A. Martínez-Huitle, M.A. Rodrigo, I. Sirés, O. Scialdone, Single and coupled electrochemical processes and reactors for the abatement of organic water pollutants: a critical review, Chem. Rev. 115 (2015) 13362–13407, http://dx.doi.org/10.1021/acs.chemrev.5b00361.

[8] E. Brillas, C.A. Martínez-Huitle, Decontamination of wastewaters containing synthetic organic dyes by electrochemical methods. An updated review, Appl. Catal. B Environ. 166 (2015) 603–643, http://dx.doi.org/10.1016/j.apcatb.2014.11.016.

[9] I. Sirés, E. Brillas, M.A. Oturan, M.A. Rodrigo, M. Panizza, Electrochemical advanced oxidation processes: today and tomorrow. A review, Environ. Sci. Pollut. Res. Int. 21 (2014) 8336–8367, http://dx.doi.org/10.1007/s11356-014-2783-1.

[10] J. Radjenovic, D.L. Sedlak, Challenges and opportunities for electrochemical processes as next-generation technologies for the treatment of contaminated water, Environ. Sci. Technol. 49 (2015) 11292–11302, http://dx.doi.org/10.1021/acs.est.5b02414.

[11] B.P. Chaplin, Critical review of electrochemical advanced oxidation processes for water treatment applications, Environ. Sci. Process. Impacts 16 (2014) 1182–1203.

[12] A. Kapałka, G. Fóti, C. Comninellis, The importance of electrode material in environmental electrochemistry: formation and reactivity of free hydroxyl radicals on boron-doped diamond electrodes, Electrochim. Acta. 54 (2009) 2018–2023, http://dx.doi.org/10.1016/j.electacta.2008.06.045.

[13] L. Labiadh, A. Barbucci, M.P. Carpanese, A. Gadri, S. Ammar, M. Panizza, Comparative depollution of methyl orange aqueous solutions by electrochemical incineration using $TiRuSnO_2$, BDD and PbO_2 as high oxidation power anodes, J. Electroanal. Chem. 766 (2016) 94–99, http://dx.doi.org/10.1016/j.jelechem.2016.01.036.

[14] J.R. Smith, F.C. Walsh, R.L. Clarke, Electrodes based on Magnéli phase titanium oxides: the properties and applications of Ebonex® materials, J. Appl. Electrochem. 28 (1998) 1021–1033, http://dx.doi.org/10.1023/A:1003469427858.

[15] P. Geng, J. Su, C. Miles, C. Comninellis, G. Chen, Highly-ordered Magnéli Ti_4O_7 nanotube arrays as effective anodic material for electro-oxidation, Electrochim. Acta. 153 (2015) 316–324, http://dx.doi.org/10.1016/j.electacta.2014.11.178.

[16] A.M. Zaky, B.P. Chaplin, Porous substoichiometric TiO_2 anodes as reactive electrochemical membranes for water treatment, Environ. Sci. Technol. 47 (2013) 6554–6563, http://dx.doi.org/10.1021/es401287e.

[17] D. Bejan, E. Guinea, N.J. Bunce, On the nature of the hydroxyl radicals produced at boron-doped diamond and Ebonex® anodes, Electrochim. Acta. 69 (2012) 275–281, http://dx.doi.org/10.1016/j.electacta.2012.02.097.

[18] S.O. Ganiyu, N. Oturan, S. Raffy, M. Cretin, R. Esmilaire, E. van Hullebusch, G. Esposito, M.A. Oturan, Sub-stoichiometric titanium oxide (Ti_4O_7) as a suitable ceramic anode for electrooxidation of organic pollutants: a case study of kinetics, mineralization and toxicity assessment of amoxicillin, Water Res. 106 (2016) 171–182, http://dx.doi.org/10.1016/j.watres.2016.09.056.

[19] S.O. Ganiyu, N. Oturan, S. Raffy, G. Esposito, E.D. van Hullebusch, M. Cretin, M.A. Oturan, Use of sub-stoichiometric titanium oxide as a ceramic electrode in anodic oxidation and electro-Fenton degradation of the beta-blocker propranolol: degradation kinetics and mineralization pathway, Electrochim. Acta. 242 (2017) 344–354, http://dx.doi.org/10.1016/j.electacta.2017.05.047.

[20] S. Garcia-Segura, E. Brillas, Applied photoelectrocatalysis on the degradation of organic pollutants in wastewaters, J. Photochem. Photobiol. C Photochem. Rev. 31

(2017) 1–35, http://dx.doi.org/10.1016/J.JPHOTOCHEMREV.2017.01.005.
[21] E. Brillas, I. Sirés, M.A. Oturan, Electro-Fenton process and related electrochemical technologies based on Fenton's reaction chemistry, Chem. Rev. 109 (2009) 6570–6631, http://dx.doi.org/10.1021/cr900136g.
[22] O. García-Rodríguez, J.A. Bañuelos, A. El-Ghenymy, L.A. Godínez, E. Brillas, F.J. Rodríguez-Valadez, Use of a carbon felt–iron oxide air-diffusion cathode for the mineralization of malachite green dye by heterogeneous electro-Fenton and UVA photoelectro-Fenton processes, J. Electroanal. Chem. 767 (2016) 40–48, http://dx.doi.org/10.1016/j.jelechem.2016.01.035.
[23] G. Santana-Martínez, G. Roa-Morales, E. Martin del Campo, R. Romero, B.A. Frontana-Uribe, R. Natividad, Electro-Fenton and electro-Fenton-like with in situ electrogeneration of H_2O_2 and catalyst applied to 4-chlorophenol mineralization, Electrochim. Acta. 195 (2016) 246–256, http://dx.doi.org/10.1016/j.electacta.2016.02.093.
[24] L. Ma, M. Zhou, G. Ren, W. Yang, L. Liang, A highly energy-efficient flow-through electro-Fenton process for organic pollutants degradation, Electrochim. Acta. 200 (2016) 222–230, http://dx.doi.org/10.1016/j.electacta.2016.03.181.
[25] H. Zazou, N. Oturan, M. Sönmez-Çelebi, M. Hamdani, M.A. Oturan, Mineralization of chlorobenzene in aqueous medium by anodic oxidation and electro-Fenton processes using Pt or BDD anode and carbon felt cathode, J. Electroanal. Chem. 774 (2016) 22–30, http://dx.doi.org/10.1016/j.jelechem.2016.04.051.
[26] T.X.H. Le, M. Bechelany, S. Lacour, N. Oturan, M.A. Oturan, M. Cretin, High removal efficiency of dye pollutants by electron-Fenton process using a graphene based cathode, Carbon N. Y. 94 (2015) 1003–1011, http://dx.doi.org/10.1016/j.carbon.2015.07.086.
[27] H. Lan, W. He, A. Wang, R. Liu, H. Liu, J. Qu, C.P. Huang, An activated carbon fiber cathode for the degradation of glyphosate in aqueous solutions by the electro-Fenton mode: optimal operational conditions and the deposition of iron on cathode on electrode reusability, Water Res. 105 (2016) 575–582, http://dx.doi.org/10.1016/j.watres.2016.09.036.
[28] T.X. Huong Le, M. Bechelany, M. Cretin, Carbon felt based-electrodes for energy and environmental applications: a review, Carbon N. Y. 122 (2017) 564–591, http://dx.doi.org/10.1016/J.CARBON.2017.06.078.
[29] N. Oturan, E. Brillas, M.A. Oturan, Unprecedented total mineralization of atrazine and cyanuric acid by anodic oxidation and electro-Fenton with a boron-doped diamond anode, Environ. Chem. Lett. 10 (2012) 165–170, http://dx.doi.org/10.1007/s10311-011-0337-z.
[30] F. Sopaj, N. Oturan, J. Pinson, F. Podvorica, M.A. Oturan, Effect of the anode materials on the efficiency of the electro-Fenton process for the mineralization of the antibiotic sulfamethazine, Appl. Catal. B Environ. 199 (2016) 331–341, http://dx.doi.org/10.1016/j.apcatb.2016.06.035.
[31] C. Gadipelly, A. Pérez-González, G.D. Yadav, I. Ortiz, R. Ibáñez, V.K. Rathod, K.V. Marathe, Pharmaceutical industry wastewater: review of the technologies for water treatment and reuse, Ind. Eng. Chem. Res. 53 (2014) 11571–11592, http://dx.doi.org/10.1021/ie501210j.
[32] O. Ganzenko, D. Huguenot, E.D. van Hullebusch, G. Esposito, M.A. Oturan, Electrochemical advanced oxidation and biological processes for wastewater treatment: a review of the combined approaches, Environ. Sci. Pollut. Res. Int. 21 (2014) 8493–8524, http://dx.doi.org/10.1007/s11356-014-2770-6.
[33] S.O. Ganiyu, E.D. van Hullebusch, M. Cretin, G. Esposito, M.A. Oturan, Coupling of membrane filtration and advanced oxidation processes for removal of pharmaceutical residues: a critical review, Sep. Purif. Technol. 156 (2015) 891–914, http://dx.doi.org/10.1016/j.seppur.2015.09.059.
[34] Y. Lan, C. Coetsier, C. Causserand, K.G. Serrano, Feasibility of micropollutants treatment by coupling nanofiltration and electrochemical oxidation: case of hospital wastewater, Int. J. Chem. React. Eng. 13 (2015) 153–159, http://dx.doi.org/10.1515/ijcre-2014-0136.
[35] N. Ma, X. Quan, Y. Zhang, S. Chen, H. Zhao, Integration of separation and photocatalysis using an inorganic membrane modified with Si-doped TiO_2 for water purification, J. Memb. Sci. 335 (2009) 58–67, http://dx.doi.org/10.1016/j.memsci.2009.02.040.
[36] A. Ronen, S.L. Walker, D. Jassby, Electroconductive and electroresponsive membranes for water treatment, Rev. Chem. Eng. 32 (2016) 533–550, http://dx.doi.org/10.1515/revce-2015-0060.
[37] X.W. Li, J.X. Li, C.Y. Gao, M. Chang, Surface modification of titanium membrane by chemical vapor deposition and its electrochemical self-cleaning, Appl. Surf. Sci. 258 (2011) 489–493, http://dx.doi.org/10.1016/j.apsusc.2011.08.083.
[38] Y. Juang, E. Nurhayati, C. Huang, J.R. Pan, S. Huang, A hybrid electrochemical advanced oxidation/microfiltration system using BDD/Ti anode for acid yellow 36 dye wastewater treatment, Sep. Purif. Technol. 120 (2013) 289–295, http://dx.doi.org/10.1016/j.seppur.2013.09.042.
[39] P. Liang, M. Rivallin, S. Cerneaux, S. Lacour, E. Petit, M. Cretin, Coupling cathodic electro-Fenton reaction to membrane filtration for AO7 dye degradation: a successful feasibility study, J. Memb. Sci. 510 (2016) 182–190, http://dx.doi.org/10.1016/j.memsci.2016.02.071.
[40] J.E. Yanez, H.Z. Wang, S. Lege, M. Obst, S. Roehler, C.J. Burkhardt, C. Zwiener, Application and characterization of electroactive membranes based on carbon nanotubes and zerovalent iron nanoparticles, Water Res. 108 (2017) 78–85, http://dx.doi.org/10.1016/j.watres.2016.10.055.
[41] P. Tao, Y. Xu, C. Song, Y. Yin, Z. Yang, S. Wen, S. Wang, H. Liu, S. Li, C. Li, T. Wang, M. Shao, A novel strategy for the removal of rhodamine B (RhB) dye from wastewater by coal-based carbon membranes coupled with the electric field, Sep. Purif. Technol. 179 (2017) 175–183, http://dx.doi.org/10.1016/j.seppur.2017.02.014.
[42] L. Tang, A. Iddya, X. Zhu, A.V. Dudchenko, W. Duan, C. Turchi, J. Vanneste, T.Y. Cath, D. Jassby, Enhanced flux and electrochemical cleaning of silicate scaling on carbon nanotube-coated membrane distillation membranes treating geothermal brines, ACS Appl. Mater. Interfaces. 9 (2017) 38594–38605, http://dx.doi.org/10.1021/acsami.7b12615.
[43] P. Geng, G. Chen, Antifouling ceramic membrane electrode modified by Magnéli Ti_4O_7 for electro-microfiltration of humic acid, Sep. Purif. Technol. 185 (2017) 61–71, http://dx.doi.org/10.1016/j.seppur.2017.05.023.
[44] A.M. Zaky, B.P. Chaplin, Mechanism of p-substituted phenol oxidation at a Ti_4O_7 reactive electrochemical membrane, Environ. Sci. Technol. 48 (2014) 5857–5867, http://dx.doi.org/10.1021/es5010472.
[45] W.N.W. Salleh, A.F. Ismail, Carbon membranes for gas separation processes: recent progress and future perspective, J. Membr. Sci. Res. 1 (2015) 2–15.
[46] C. Li, C. Song, P. Tao, M. Sun, Z. Pan, T. Wang, M. Shao, Enhanced separation performance of coal-based carbon membranes coupled with an electric field for oily wastewater treatment, Sep. Purif. Technol. 168 (2016) 47–56, http://dx.doi.org/10.1016/j.seppur.2016.05.020.
[47] J. Zheng, J. Ma, Z. Wang, S. Xu, T.D. Waite, Z. Wu, Contaminant removal from source waters using cathodic electrochemical membrane filtration: mechanisms and implications, Environ. Sci. Technol. 51 (2017) 2757–2765, http://dx.doi.org/10.1021/acs.est.6b05625.
[48] E. Brillas, E. Mur, J. Casado, Iron(II) catalysis of the mineralization of aniline using a carbon-PTFE O[sub 2]-fed cathode, J. Electrochem. Soc. 143 (1996) L49, http://dx.doi.org/10.1149/1.1836528.
[49] O. Scialdone, A. Galia, C. Gattuso, S. Sabatino, B. Schiavo, Effect of air pressure on the electro-generation of H_2O_2 and the abatement of organic pollutants in water by electro-Fenton process, Electrochim. Acta. 182 (2015) 775–780, http://dx.doi.org/10.1016/j.electacta.2015.09.109.
[50] T.X.H. Le, M. Bechelany, J. Champavert, M. Cretin, A highly active based graphene cathode for the electro-Fenton reaction, RSC Adv. 5 (2015) 42536–42539, http://dx.doi.org/10.1039/C5RA04811G.
[51] T.X.H. Le, R. Esmilaire, M. Drobek, M. Bechelany, C. Vallicari, S. Cerneaux, A. Julbe, M. Cretin, Nitrogen-doped graphitized carbon electrodes for biorefractory pollutant removal, J. Phys. Chem. C. 121 (2017) 15188–15197, http://dx.doi.org/10.1021/acs.jpcc.7b03100.
[52] D. Nematollahi, H. Shayani-Jam, M. Alimoradi, S. Niroomand, Electrochemical oxidation of acetaminophen in aqueous solutions: kinetic evaluation of hydrolysis, hydroxylation and dimerization processes, Electrochim. Acta. 54 (2009) 7407–7415, http://dx.doi.org/10.1016/j.electacta.2009.07.077.
[53] E. Brillas, I. Sirés, C. Arias, P.L. Cabot, F. Centellas, R.M. Rodríguez, J.A. Garrido, Mineralization of paracetamol in aqueous medium by anodic oxidation with a boron-doped diamond electrode, Chemosphere 58 (2005) 399–406, http://dx.doi.org/10.1016/j.chemosphere.2004.09.028.
[54] N. Villota, J.M. Lomas, L.M. Camarero, Study of the paracetamol degradation pathway that generates color and turbidity in oxidized wastewaters by photo-Fenton technology, J. Photochem. Photobiol. A Chem. 329 (2016) 113–119, http://dx.doi.org/10.1016/J.JPHOTOCHEM.2016.06.024.
[55] E. Moctezuma, E. Leyva, C.A. Aguilar, R.A. Luna, C. Montalvo, Photocatalytic degradation of paracetamol: intermediates and total reaction mechanism, J. Hazard. Mater. 243 (2012) 130–138, http://dx.doi.org/10.1016/j.jhazmat.2012.10.010.
[56] L.C. Almeida, S. Garcia-Segura, N. Bocchi, E. Brillas, Solar photoelectro-Fenton degradation of paracetamol using a flow plant with a Pt/air-diffusion cell coupled with a compound parabolic collector: process optimization by response surface methodology, Appl. Catal. B Environ. 103 (2011) 21–30, http://dx.doi.org/10.1016/j.apcatb.2011.01.003.
[57] K. Waterston, J.W. Wang, D. Bejan, N.J. Bunce, Electrochemical waste water treatment: electrooxidation of acetaminophen, J. Appl. Electrochem. 36 (2006) 227–232, http://dx.doi.org/10.1007/s10800-005-9049-z.
[58] M.A. Oturan, M. Pimentel, N. Oturan, I. Sirés, Reaction sequence for the mineralization of the short-chain carboxylic acids usually formed upon cleavage of aromatics during electrochemical Fenton treatment, Electrochim. Acta. 54 (2008) 173–182, http://dx.doi.org/10.1016/j.electacta.2008.08.012.
[59] S. Garcia-Segura, E. Brillas, Mineralization of the recalcitrant oxalic and oxamic acids by electrochemical advanced oxidation processes using a boron-doped diamond anode, Water Res. 45 (2011) 2975–2984, http://dx.doi.org/10.1016/j.watres.2011.03.017.
[60] H. Olvera-Vargas, N. Oturan, D. Buisson, M.A. Oturan, A coupled Bio-EF process for mineralization of the pharmaceuticals furosemide and ranitidine: feasibility assessment, Chemosphere 155 (2016) 606–613, http://dx.doi.org/10.1016/j.chemosphere.2016.04.091.
[61] C. Trellu, O. Ganzenko, S. Papirio, Y. Pechaud, N. Oturan, D. Huguenot, E.D. van Hullebusch, G. Esposito, M.A. Oturan, Combination of anodic oxidation and biological treatment for the removal of phenanthrene and tween 80 from soil washing solution, Chem. Eng. J. 306 (2016) 588–596, http://dx.doi.org/10.1016/j.cej.2016.07.108.
[62] H. Olvera-Vargas, C. Trellu, N. Oturan, M.A. Oturan, Bio-electro-Fenton: a new combined process – principles and applications, in: M. Zhou, M.A. Oturan, I. Sires (Eds.), Electro-Fent. Process. Handb. Environ. Chem. Springer, Singapore, 2017, pp. 29–56, , http://dx.doi.org/10.1007/698 2017 53.